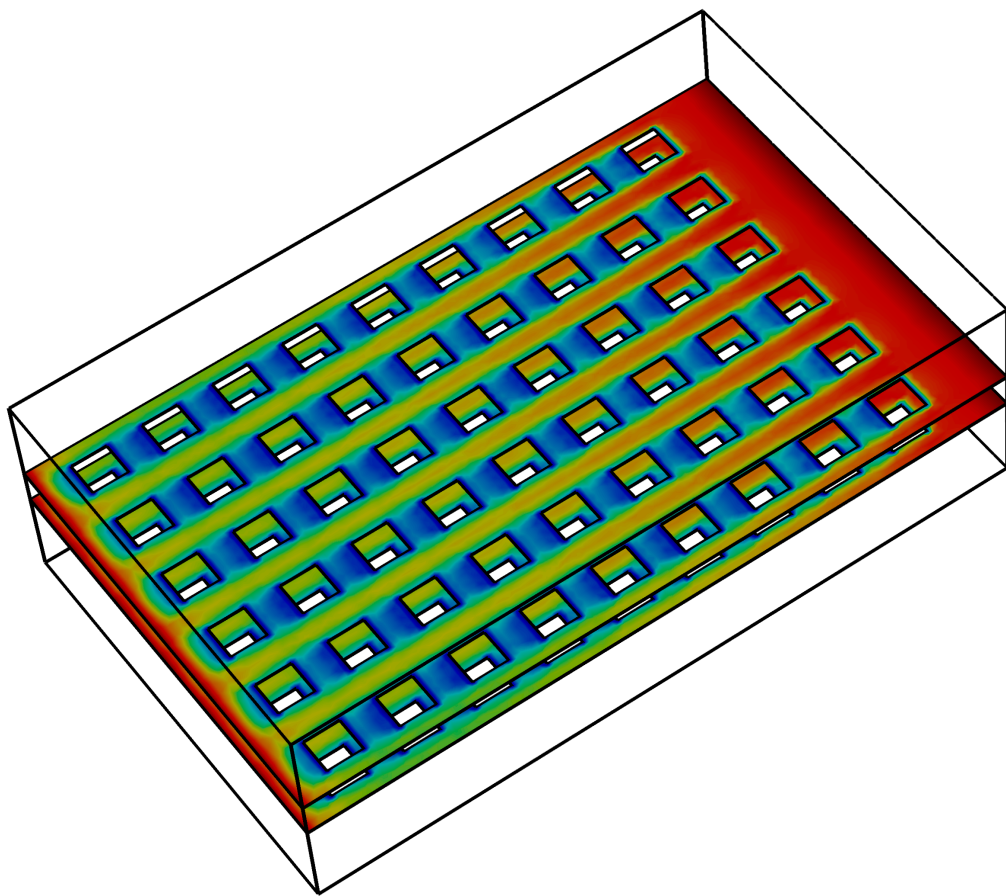


Optimization of Cleaning Methods After Coating of Nicorette[®] Chewing Gums



LUND
UNIVERSITY

Max Hammarfjord

Department of Chemical Engineering
Master Thesis 2015

Optimization of Cleaning Methods After Coating of Nicorette[®] Chewing Gums

by
Max Hammarfjord

Department of Chemical Engineering
Lund University
June 2015

Supervisor: **Ph.D. Anders Holmqvist**

Co-supervisor: **Åsa Ahlqvist**

Examiner: **Professor Bernt Nilsson**

Postal address

P.O. Box 124
SE-221 00

Web address

www.chemeng.lth.se

Visiting address

Getingevägen 60
Lund, Sweden

Telephone

+46 46-222 82 85
+46 46-222 00 00

Telefax

+46 46-222 45 26

Preface

Five years of study has brought me to this point. I have been lucky enough to claim such an interesting project at McNeil AB and collaborating with the Department of Chemical Engineering at Lund University. I hope that this report fulfills the task given and aids in the understanding of the existing cleaning process and provides some new insights into how this process might be improved.

Abstract

The cleaning methods after the coating of Nicorette® gums has a few shortcomings. The build-up of residual titanium dioxide on the walls inside the mixer and holding tank is a longstanding issue that needs to be addressed. Another issue in the cleaning process is residual gums in the pan after emptying. These residual gums may interfere and cause a mix-up with the next batch.

The current method of cleaning the mixer and holding tank between batches involves water and various detergents. This approach has shown to be ineffective in removing the titanium dioxide and new ways of eliminating these residues are warranted. It has been shown in other areas that ultrasonic cleaning methods can be an effective method in cleaning various surfaces. Ultrasonic cleaning methods have the added advantage of avoiding using other chemicals in the processes. This project evaluate whether ultrasonic cleaning could be used instead of detergents in removing titanium dioxide. Herein we show that ultrasonic cleaning removes titanium dioxide effectively. Furthermore, our experimental method also suggests that ultrasonic method may be a more time-efficient approach.

To clear the pan from residual gums, a process of combining a manual and automated approach is used. This involves a warm and cold fluid phase using a spraying method. We hypothesized that introducing a soaking phase in the rotating pan may improve the clearing of residual gums. This was investigated by simulation using COMSOL Multiphysics and the simulation data obtained suggest that a soaking phase may improve the removal of the gums. However, this modification remains to be assessed in an experimental setting.

Table of contents

Preface.....	3
Abstract	4
1 Introduction.....	6
1.1 Rotating drum	6
1.2 Titanium dioxide	7
2 Theory.....	8
2.1 Fluid profile optimization	8
2.2 Spray configuration	8
2.3 Ultrasonic cleaning	8
3 Materials and methods	9
3.1 Initial ideas.....	9
3.2 COMSOL Multiphysics.....	9
3.2.1 Assumptions	10
3.2.2 Creating the model	10
3.3 Ultrasonic cleaning on steel plates.....	11
4 Results	13
4.1 Fluid profile.....	13
4.2 Cleaning results.....	14
5 Discussion	15
6 Reference list.....	16
Acknowledgement.....	17
Appendices	18
A- COMSOL, soaking phase, page 19-35.....	18
B- COMSOL, spraying phase, page 36-52.....	18

1 Introduction

McNeil AB is the second largest private employer in Helsingborg, Sweden, and is a member of Johnson & Johnson group. In Helsingborg lies the production site for Nicorette[®], which is a central product line in the company of McNeil AB. Nicorette[®] is the world leading product used for nicotine replacement therapy (NRT). Success rates in smoking cessation has been shown to be increased with 50-70% using NRT regardless of delivery method^[1]. Thus, Nicorette[®] is a key component in helping people stop smoking.

The production of Nicorette[®] chewing gums follows good manufacturing practice (GMP). This is to ensure a high quality and safety for the consumer. To ensure that the process follows the GMP protocol, the cleaning has to be inspected manually after each campaign. At the moment there is a risk of finding remaining gums in the pan and visible titanium dioxide covering the walls of the mixer and holding tanks. The purpose of this thesis is to evaluate methods that aim to prevent the current problems from occurring, and to assess the efficiency of the current cleaning methods to try to find ways to improve the existing process.

The chewing gums consist of a gum core, which is coated with a solution containing titanium dioxide and xylitol. The solution is prepared in a mixer and stored in a holding tank before entering the rotating drum via the spray balls onto the gums.

1.1 Rotating drum

The coating process of Nicorette[®] chewing gums consists of a rotating drum with a spray arm in the center where the coating solution and suspension are distributed. The solution enters the drum through the nozzles of the spray arm that also are used during the cleaning process. A simplified illustration of the rotating drum is shown in figure 1 below.

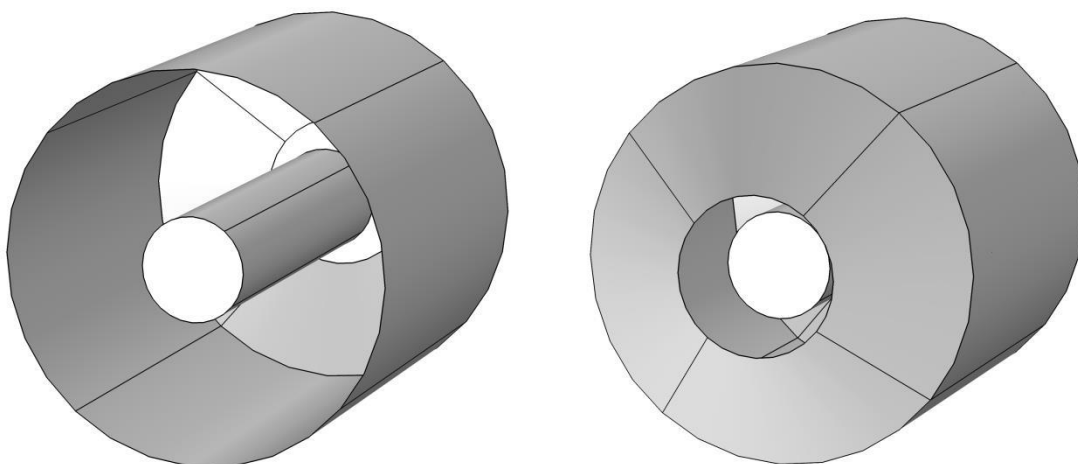


Figure 1: Rotating drum, with and without the front wall. The spray arm is shown as the cylinder in the middle.

A few plastic tubes are connected to the nozzles on the spray arm. The tubes are not integrated in the structure which enables easy access when replacing any damaged equipment. However, this design allows gums to get trapped between the tubes.

The coating solution consists of a xylitol-mixture with titanium dioxide and different types of flavor depending of the current campaign. Blowing hot air into the drum dries the gums and afterwards the gums exit the rotating drum. Excess of gums are manually removed and the automatic cleaning phase begins.

The cleaning process introduces cold water to remove any excess gums from the production. The cold water is used to prevent the gums from melting and get stuck onto the walls. If there are gums remaining after the cold water cycle, the gums will melt and get stuck during the warm water phase. The drum is cleaned with hot water and detergent and afterwards rinsed with water to remove any remaining detergent.

1.2 Titanium dioxide

Titanium dioxide (TiO_2) is used as whitening pigment on the gums due to the light scattering characteristics of the TiO_2 -crystals^[4]. Its insolubility in water and stability at low temperatures make it challenging to remove the particles once they have been adhered to the walls of the mixer and holding tank. Water can however be adsorbed on the surface of the TiO_2 -crystals^[3], so it could be possible to introduce a detergent that adsorbs on the surface but interacts more strongly with the water than the TiO_2 -interaction with the wall. However, the current detergent is not effective enough, so for the time being it is removed manually after which the level TiO_2 present on the walls is assessed visually.

There are two major problems with manually removing the pigment. Firstly, there are health and safety aspects of breathing in the dust particles that are formed. Secondly, it is time-consuming and therefore increases the cost of production. However, since the pigment can be removed manually, a physical cleaning approach might be preferred over finding new suitable chemicals.

2 Theory

2.1 Fluid profile optimization

By increasing the water flow against the remaining gums during the cold water cycle, the current cleaning process might improve. This could be achieved by introducing a soaking stage during the phase, without increasing the water amount and without investing in new pumps. This could be performed by stopping the outflow and filling the bottom of the drum with water so that the wall has to rotate through the liquid phase at the bottom during the cycle, as illustrated in figure 2 below.

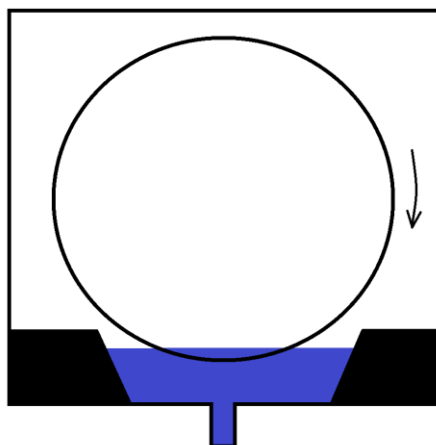


Figure 2: Illustration of a possible soaking stage for the rotating drum.

The soaking stage would not necessarily increase the pressure but would use the rotation of the drum to create a new fluid profile that changes the pressure vectors and therefore increasing the number of possible directions for initializing gum movement.

2.2 Spray configuration

The current process uses spray balls, which cover the whole drum. By shifting to a flat spray pattern the pressure can be focused on a single segment and since the drum already rotates, all the walls will be covered nonetheless. Furthermore, the current spray ball located closest to the exit could disrupt the flow of the remaining gums from leaving the pan, keeping them rotating along the wall and can therefore not be elevated enough to reach the exit. This speculation is based on the observation that most of the residual gums ends up near the exit.

2.3 Ultrasonic cleaning

Ultrasound could be an option for removing the TiO_2 from the walls. Ultrasound works by generating microscopic bubbles in the water that implodes due to cavitation^[2]. The cavitation produces kinetic motion that disperses the titanium dioxide as fine particles that desorbs from the wall and can therefore flow with the water.

The conventional way of using ultrasonic cleaning is to place the object in an ultrasonic bath, however this method would not work when cleaning a large tank. Nevertheless, there are solutions where the energy source can be placed inside of the tank and emitting the sound-waves outwards but would require further research.

3 Materials and methods

3.1 Initial ideas

At the start, a couple of different ideas were discussed and evaluated before deciding what to test. The first suggestion was to use glass or plastic beads in the process to physically scrape the pigment of the walls during the cleaning cycle. However, this method would not be suitable for use in the holding tank and mixer. Only in the rotating drum where the TiO₂ is not an issue would this method be viable. Nonetheless it would have similar effects against the pigment as the gums already have.

Another method proposed was to rearrange the currently used spray balls or changing the spray equipment completely. The currently used cleaning in place could be efficient enough just by changing to more effective spray equipment. Nevertheless, this could not be tested in the facility without a proper investigation of the matter since it would halt the production. To examine how the spray balls affect the flow and pressure profile in the drum, a simulation in COMSOL Multiphysics was made. However, since the model had to be made of two phases, assuming water and air, the computation time exceeded the total length of this project. The computation time was cut by assuming a two-dimensional plane that could be rotated, instead of using a three-dimensional model. The model was further simplified with the help of COMSOL technical support. However, the simulation was still far too time-consuming to be of use.

3.2 COMSOL Multiphysics

The fluid profiles against the wall of the rotating drum were modeled in COMSOL Multiphysics. A small sample of the meshed wall was assumed to represent the drum as a whole to simplify the calculations and thus lowering the computing time. The steel wall is constructed with a regular pattern of holes for the water to exit through. The pattern of holes is not placed exactly as on the actual wall, due to the need for further simplification, however these simplifications used to enable the modulation is not expected to significantly affect the data obtained.

The model is single phased with water as the component, assuming for both soaking and spray phase. The drum completes approximately three rotations per minute and therefore the wall velocity through the water is estimated to 0.5 m/s. However, the model is made so that the wall is stationary and the water is moving.

Since water is listed in COMSOL, the fluid properties are taken from materials, which is the list function of the program for specific materials. The model was constructed into two parts, one concerning the soaking phase and the other for the current spray phase; both are fully listed in the appendix.

The geometry was created by using blocks to make a box, as seen in figure 3, which is filled with water and a meshed wall in the middle which illustrates the wall of the drum.

3.2.1 Assumptions

- Changes in the fluid profile against the wall increase the number of variables for the system, which is more important than the actual values.
- The changes carry over between the systems in a similar fashion.
- The space closest to the wall contains water, even during the spray phase.

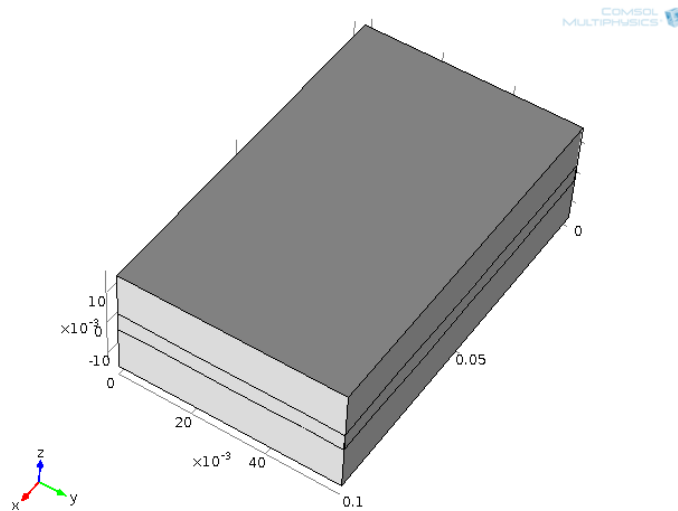


Figure 3: The model geometry of the wall segment, created in COMSOL Multiphysics.

3.2.2 Creating the model

The model is designed in three dimensions where the mathematics that describes the flow considers turbulent effects. The simulation of the model is chosen as a stationary study, which reduces the computation time compared to when applying a time-dependent study. A stationary study generates an average flow pattern for the model which can be used to find differences between the two cases.

The equation that describes the model in COMSOL is based on Reynolds-Averaged Navier-stokes (RANS) formulation for k-epsilon. The RANS approximates the turbulent effects by producing a time-average of the local oscillations in the flow. With k-epsilon, the model solves two variables, k; the turbulent kinetic energy, and epsilon; the rate of dissipation of kinetic energy.

The geometry is selected, as shown in figure 3, where two water filled chambers is separated by a solid meshed wall. The in-flow and out-flow is alternated to create the different models. For the soaking phase, the in- and out-flow is located on the short sides of the box, and for the spraying phase, the flow is located on the top and the bottom. The flow velocity is fixed to 0.5 m/s for both cases which supports a simple way of comparing the two methods.

3.3 Ultrasonic cleaning on steel plates

To test if the ultrasonic cleaning method could be used to remove TiO_2 from the walls, the following experiment was designed and performed.

10x10 cm of stainless steel plates were contaminated with the solution containing TiO_2 . This resulted in a white color on the sheets, as seen in figure 4. Afterwards, the plates were left over night to dry in an oven set to 50°C to match the process conditions and replicate the problem.

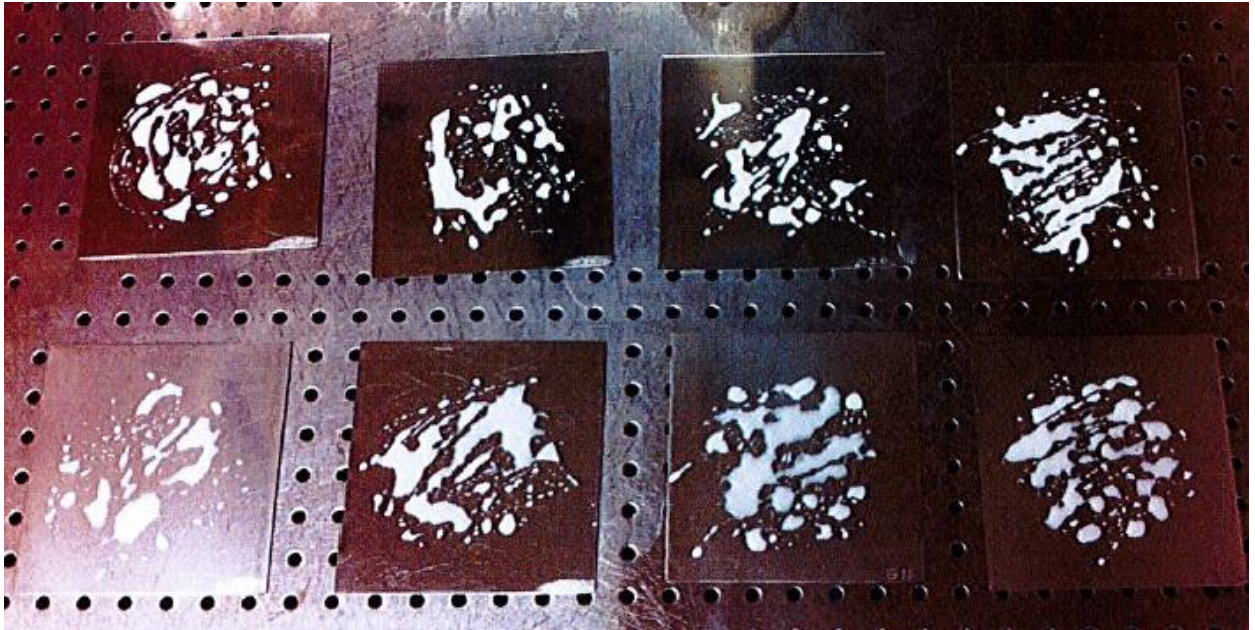


Figure 4: Steel plates contaminated with the solution containing titanium dioxide.

The first steel plates were lowered halfway down a beaker of water with a magnetic stirrer for 30 minutes, as seen in on the left side of figure 5 on the next page. No detergents were used during the experiments. However, since the detergents that are used in the cleaning process of the mixer and drum do not remove the TiO_2 we assumed that water would be suitable as a control.

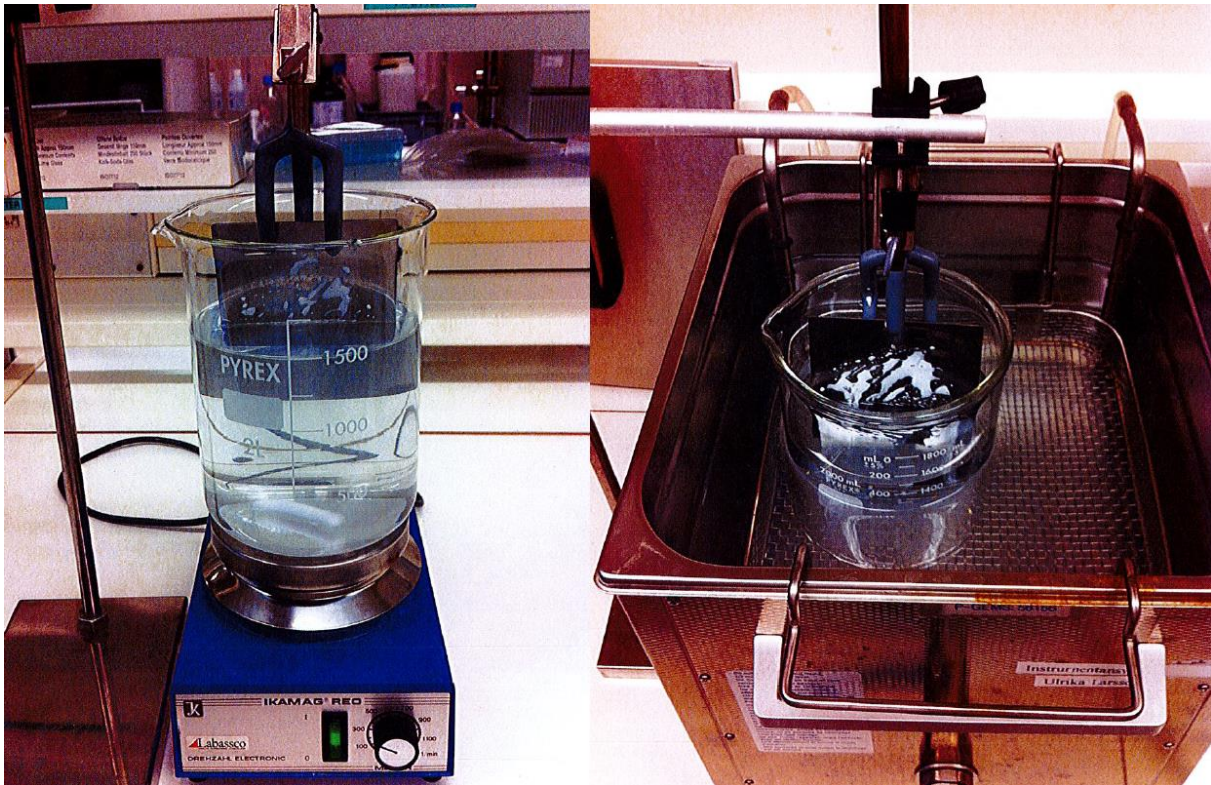


Figure 5: The arrangements of the different cleaning methods.

The remaining steel plates were tested in an ultrasonic cleaning bath by the same technique. We found that the ultrasonic cleaning method appeared to be effective already after 10 minutes and therefore removed the plates prematurely compared to the first experiment. The plates were visually inspected, assessed, and photographed for documentation. The arrangement can be seen on the right side in figure 5.

4 Results

4.1 Fluid profile

The model of the soaking stage showed that the velocity near the wall flows with the pattern of the wall. A higher velocity increases the shear stress near the wall and increases the force on a gum that is stuck on the wall. This variance in fluid velocity in various regions is shown by the coloring of figure 6 below. A complete image can be found in the appendix, which however contains effects from the stationary walls on the side that should not be accounted for in a larger system. Because of this, the two images below are cut out from the center piece of each model for a more realistic perspective.

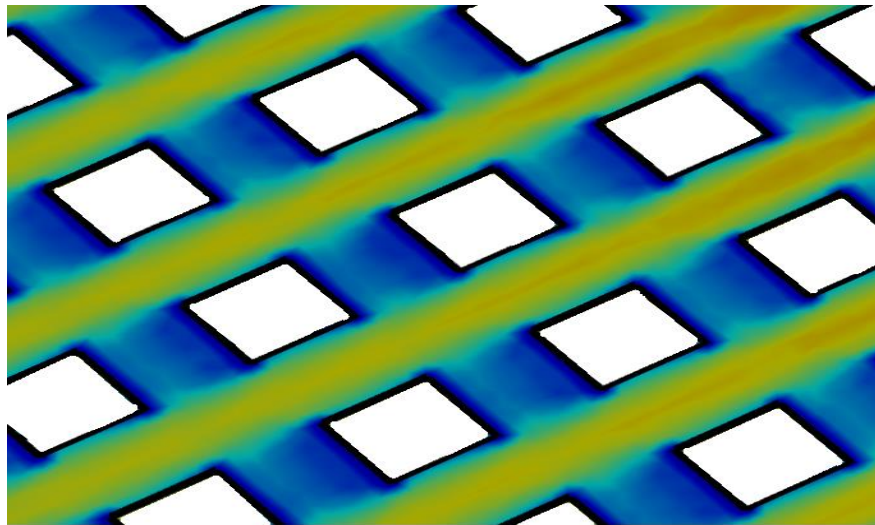


Figure 6: Fluid profile during soaking phase.

The velocity ranges from 0 to 0.25 m/s going from blue (slow) to red (fast) scale with yellow somewhere in between. Compared to the fluid profile of the current spraying phase (shown in figure 7) there are some major differences between the both profiles.

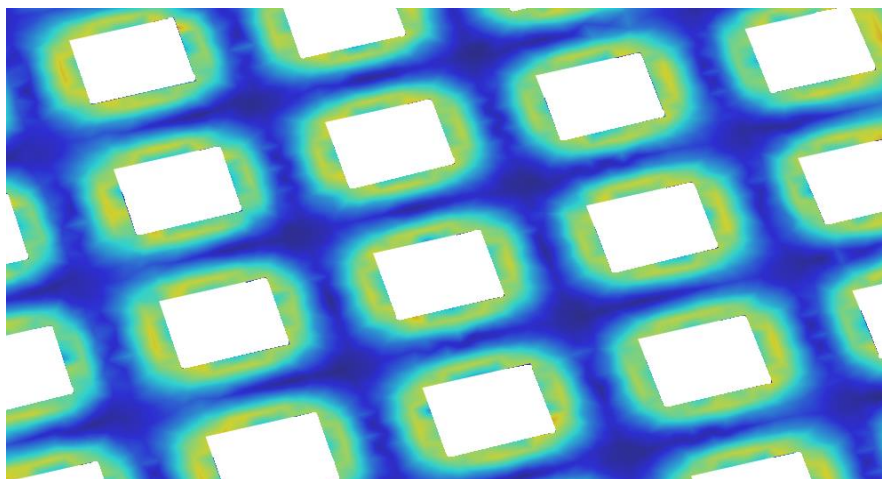


Figure 7: Fluid profile during spraying phase.

The idea is not to find that one profile is better than the other for increasing the pressure on remaining gums, but rather to implement both ways in the current process to increase the

number of variables in the system and therefore gain other velocity vectors that can work regardless of how and where the gum is bound to the surface.

By superimpose the first model on the second, both the area around the holes and between them would see an increase in pressure and therefore create a more effective way of removing residual gums.

A broader study would be of interest to investigate how different velocities can affect the fluid profile since the velocity for the spraying phase can more easily be altered. However, the velocity for the soaking phase cannot be increased much further due to restrictions of the existing equipment. Also it would be possible to insert an obstacle in the model for representing a fixed gum on the wall and look for changes in the fluid profile.

4.2 Cleaning results

By visually analyzing the plates in figure 8 below, one can see the effectiveness of the cleaning methods. The left plate was cleaned by water during agitation at 23°C for 30 minutes and there is still remaining TiO₂ visible on the lower half. However, the plate on the right that was cleaned in an ultrasonic bath at 23°C for 10 minutes shows no visual evidence of a white colored coating on the bottom half.

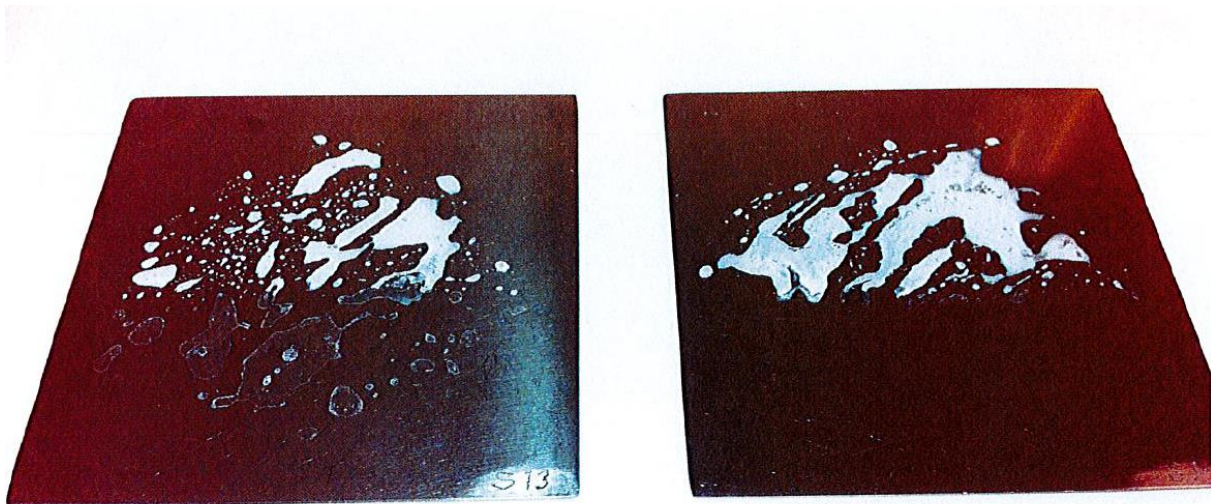


Figure 8: Results of the different cleaning methods. The regular method is shown on the left, with some coating still remaining. The ultrasonic bath method is shown on the right, with no visual traces of coating.

This experiment suggests that ultrasonic cleaning method may be an effective method in removing TiO₂ from the steel surface. The comparison of the regular method is not exactly the same as the actual process since no detergent was used. However, the plates are sufficiently clean after the ultrasonic treatment using the same assessment method as in the real process and also in a shorter amount of time as compared to the control group.

5 Discussion

The aim of this project was to investigate new methods of removing residual gum from the pan after coating and TiO_2 from the walls of the mixer and holding tank. These are two significant problems in the production of Nicorette[®] chewing gums.

The simulation performed suggests that adding a soaking phase after removing the gums would increase the number of ways pressure can be applied on individual gums. This would give rise to a more random pattern of pressure and thus yield a higher number of gums that could be removed. To enable this modification of the process the mechanical strength of the rotating drum has to be able to rotate through the water. Since it already handles the weight of the gums this is unlikely to be a problem. Nevertheless, this needs to be formally assessed.

Furthermore the simulation can be modified to include different geometrical obstacles that could represent gums on the wall, which could give rise to a more proper investigation of the pressure profile exhibited on the gums.

The configuration and type of spray equipment would also be of interest to evaluate, as the spray pattern can affect the exit route of the gums. A possible method of choice would be by remove the spray ball nearest the exit during a cleaning cycle and then evaluate whether there are gums occupying the same space as before. Another possible modification that could be worth investigating is if shielding the spray arm would prevent gums from getting stuck inside the equipment.

Fitting cameras in the rotating pan might be an alternative to remove the manual inspection completely. The cameras could be shielded by a lens that can be closed during the procedure and removed when needed. These cameras can also be placed on the spray arm to make sure that they cover all angles, except for the arm itself. However, the arm can be removed and cleaned outside of the pan if needed, but this may not be necessary if shielded properly.

This study shows that TiO_2 can be removed using an ultrasonic cleaning method. Whether the ultrasonic cleaning method would work in the mixer and holding tank remains to be assessed. This method has the advantages of not adding any new chemicals to the process and also this method is relatively fast to perform. This could potentially save time, which would increase the efficiency of the process as a whole. However, a comparison with the current detergents needs further evaluation. The data on using a ultrasonic cleaning method are promising since the outcome is a clean surface in a relatively short period of time, however further testing is needed to investigate whether it could work on a larger scale and with another type of arrangement of the energy source, i.e., where the equipment can be installed in the mixer and holding tank respectively.

6 Reference list

- 1 L.F. Stead et al. *Cochrane Database Syst Rev.* 2012 Nov 14;11:CD000146.
doi: 10.1002/14651858.CD000146.pub4.
- 2 A.D. Farmer, A. C. (2000). The application of power ultrasound to the surface cleaning of silica. *Ultrasonics Sonochemistry*, 243-427.
- 3 Diebold, U. (2003). The surface science of titanium dioxide. *Surface Science Reports* 48, 53-229.
- 4 Bolt, J. D. (1997). *USA Patent No. 5,650,002.*

Acknowledgement

I would like to thank McNeil AB for giving me the opportunity to work with such an interesting project and for the warm welcome and treatment during my thesis.

A special thanks to Åsa Ahlqvist for all the support and guidance. Also Giulia Toncelli for all the help and explanations of how the process works. Also I would like to thank Anders Holmberg for all the experiments performed at McNeil.

I would also like to thank Professor Bernt Nilsson for being a source of inspiration. Anders Holmqvist for being a true master in COMSOL, and for the support during the project as a whole.

Appendices

- A- COMSOL, soaking phase, page 19-35
- B- COMSOL, spraying phase, page 36-52

A- COMSOL, soaking phase

1	Component 1 (comp1)	20
1.1	Definitions	20
1.2	Geometry 1	20
1.3	Materials	21
1.4	Turbulent Flow, k- ϵ (spf)	22
1.5	Mesh 1	29
2	Study 1	30
2.1	Stationary	30
2.2	Solver Configurations	30
3	Results	34
3.1	Plot Groups	34

1 Component 1 (comp1)

1.1 Definitions

1.1.1 Coordinate Systems

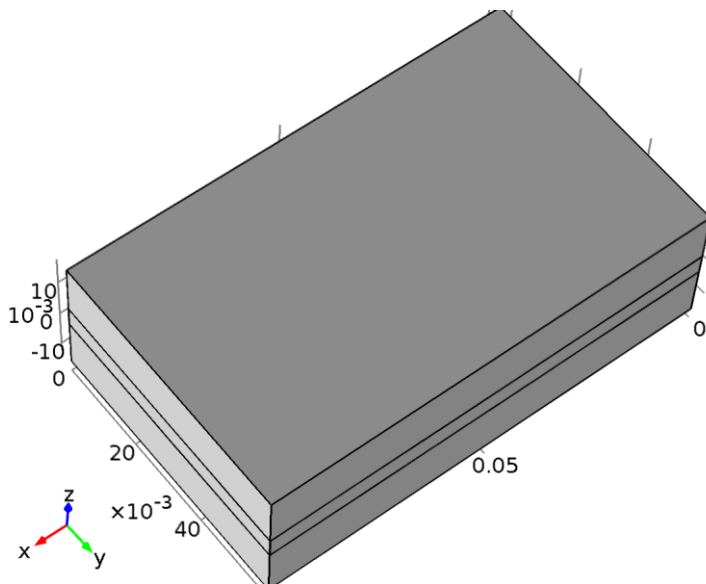
Boundary System 1

Coordinate system type	Boundary system
Identifier	sys1

Settings

Name	Value
Coordinate names	{t1, t2, n}
Create first tangent direction from	Global Cartesian

1.2 Geometry 1



Geometry 1

Units

Length unit	m
Angular unit	deg

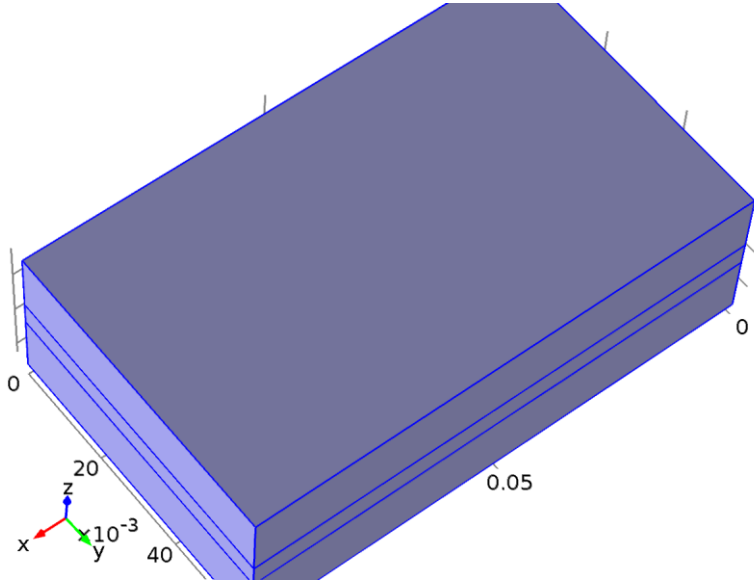
Geometry statistics

Property	Value
Space dimension	3
Number of domains	2
Number of boundaries	232

Property	Value
Number of edges	676
Number of vertices	448

1.3 Materials

1.3.1 Water



Water

Selection

Geometric entity level	Domain
Selection	Domains 1–2

Material parameters

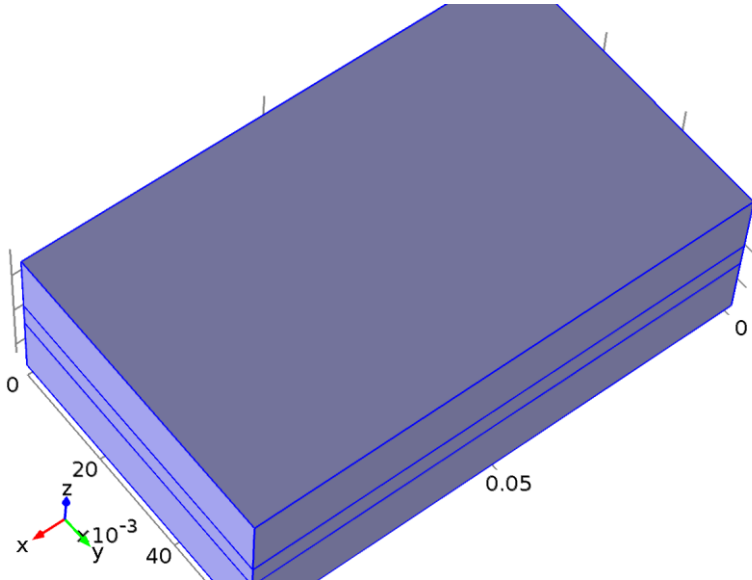
Name	Value	Unit
Dynamic viscosity	$\eta(T[1/K])[\text{Pa}\cdot\text{s}]$	$\text{Pa}\cdot\text{s}$
Density	$\rho(T[1/K])[\text{kg}/\text{m}^3]$	kg/m^3

Basic Settings

Description	Value
Dynamic viscosity	$\eta(T[1/K])[\text{Pa}\cdot\text{s}]$
Ratio of specific heats	1.0
Electrical conductivity	$\{\{5.5\text{e-}6[\text{S}/\text{m}], 0, 0\}, \{0, 5.5\text{e-}6[\text{S}/\text{m}], 0\}, \{0, 0, 5.5\text{e-}6[\text{S}/\text{m}]\}\}$
Heat capacity at constant pressure	$C_p(T[1/K])[\text{J}/(\text{kg}\cdot\text{K})]$
Density	$\rho(T[1/K])[\text{kg}/\text{m}^3]$

Description	Value
Thermal conductivity	{{k(T[1/K])[W/(m*K)], 0, 0}, {0, k(T[1/K])[W/(m*K)], 0}, {0, 0, k(T[1/K])[W/(m*K)]}}
Speed of sound	cs(T[1/K])[m/s]

1.4 Turbulent Flow, k-ε (spf)



Turbulent Flow, k-ε

Selection

Geometric entity level	Domain
Selection	Domains 1–2

Equations

$$\rho(\mathbf{u} \cdot \nabla)\mathbf{u} = \nabla \cdot \left[-p\mathbf{I} + \left(\mu + \mu_T \right) (\nabla\mathbf{u} + (\nabla\mathbf{u})^T) - \frac{2}{3}(\mu + \mu_T)(\nabla \cdot \mathbf{u})\mathbf{I} - \frac{2}{3}\rho k\mathbf{I} \right] + \mathbf{F}$$

$$\nabla \cdot (\rho\mathbf{u}) = 0$$

$$\rho(\mathbf{u} \cdot \nabla)k = \nabla \cdot \left[\left(\mu + \frac{\mu_T}{\sigma_k} \right) \nabla k \right] + P_k - \rho\epsilon$$

$$\rho(\mathbf{u} \cdot \nabla)\epsilon = \nabla \cdot \left[\left(\mu + \frac{\mu_T}{\sigma_\epsilon} \right) \nabla \epsilon \right] + C_{\epsilon 1} \frac{\epsilon}{k} P_k - C_{\epsilon 2} \rho \frac{\epsilon^2}{k}, \quad \epsilon = \text{ep}$$

$$\mu_T = \rho C_\mu \frac{k^2}{\epsilon}$$

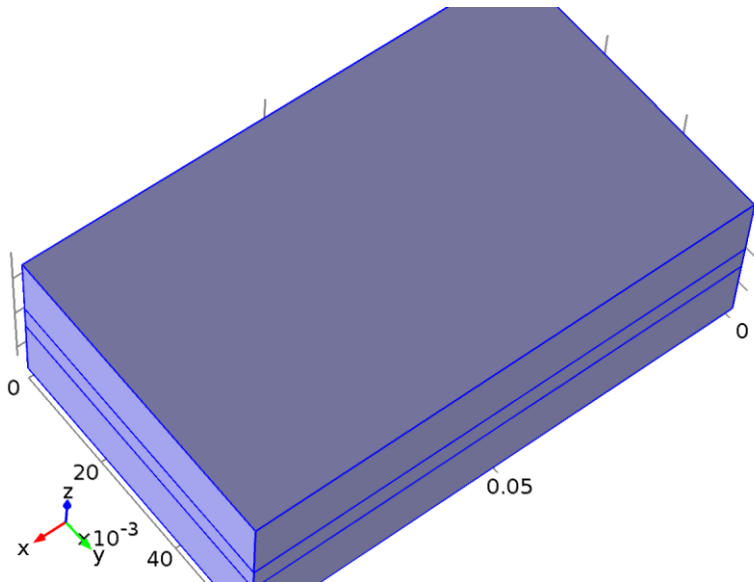
$$P_k = \mu_T \left[\nabla\mathbf{u} : (\nabla\mathbf{u} + (\nabla\mathbf{u})^T) - \frac{2}{3}(\nabla \cdot \mathbf{u})^2 \right] - \frac{2}{3}\rho k \nabla \cdot \mathbf{u}$$

Settings

Description	Value
Discretization of fluids	P1 + P1

Description	Value
Value type when using splitting of complex variables	{Real, Real, Real, Real, Real, Real, Real, Real, Real, Real}

1.4.1 Fluid Properties 1



Fluid Properties 1

Selection

Geometric entity level	Domain
Selection	Domains 1–2

Equations

$$\rho(\mathbf{u} \cdot \nabla)\mathbf{u} = \nabla \cdot \left[-p\mathbf{I} + (\mu + \mu_T)(\nabla\mathbf{u} + (\nabla\mathbf{u})^T) - \frac{2}{3}(\mu + \mu_T)(\nabla \cdot \mathbf{u})\mathbf{I} - \frac{2}{3}\rho\mathbf{k}\mathbf{l} \right] + \mathbf{F}$$

$$\nabla \cdot (\rho\mathbf{u}) = 0$$

$$\rho(\mathbf{u} \cdot \nabla)k = \nabla \cdot \left[\left(\mu + \frac{\mu_T}{\sigma_k} \right) \nabla k \right] + P_k - \rho\epsilon$$

$$\rho(\mathbf{u} \cdot \nabla)\epsilon = \nabla \cdot \left[\left(\mu + \frac{\mu_T}{\sigma_\epsilon} \right) \nabla \epsilon \right] + C_{d1} \frac{\epsilon}{k} P_k - C_{d2} \rho \frac{\epsilon^2}{k}, \quad \epsilon = \text{ep}$$

Settings

Settings

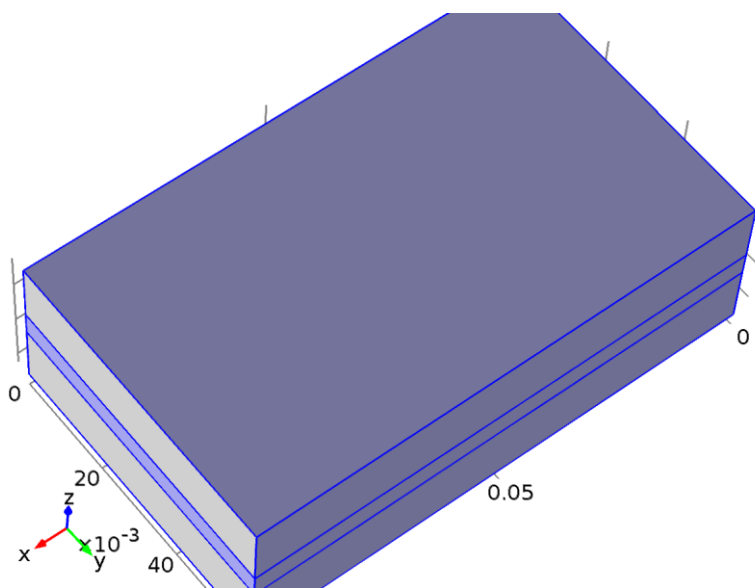
Description	Value
Density	From material
Dynamic viscosity	From material

Description	Value
Reference length	1
Reference length scale	Automatic
Mixing length limit	Automatic

Properties from material

Property	Material	Property group
Density	Water	Basic
Dynamic viscosity	Water	Basic

1.4.2 Wall 1



Wall 1

Selection

Geometric entity level	Boundary
Selection	Boundaries 2–5, 8, 10–13, 231

Equations

$$\mathbf{u} \cdot \mathbf{n} = 0$$

$$\left[(\mu + \mu_T)(\nabla \mathbf{u} + (\nabla \mathbf{u})^T) - \frac{2}{3}(\mu + \mu_T)(\nabla \cdot \mathbf{u})\mathbf{I} - \frac{2}{3}\rho k \mathbf{I} \right] \mathbf{n} = -\rho \frac{u_\tau}{\delta_w^+} \mathbf{u}_{\text{tang}}$$

$$\mathbf{u}_{\text{tang}} = \mathbf{u} - (\mathbf{u} \cdot \mathbf{n})\mathbf{n}$$

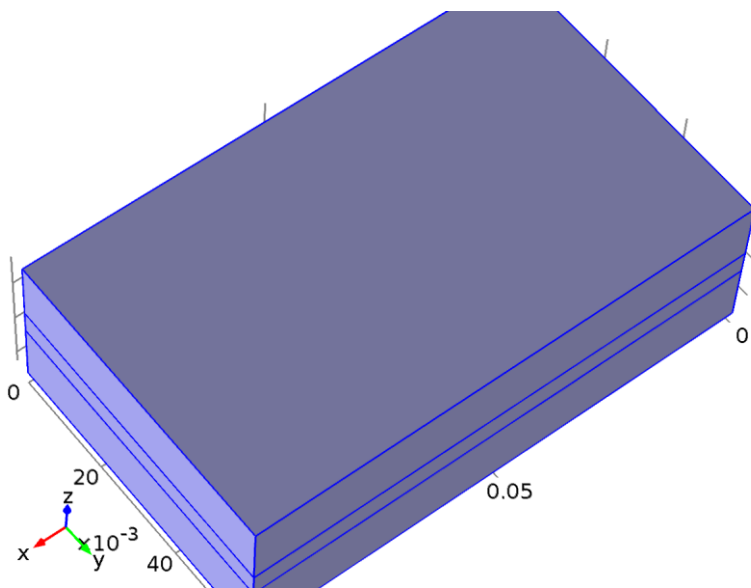
$$\nabla k \cdot \mathbf{n} = 0, \quad \epsilon = \rho \frac{C_\mu k^2}{\kappa_v \delta_w^+ \mu}$$

Settings

Settings

Description	Value
Temperature	User defined
Temperature	293.15[K]
Electric field	User defined
Electric field	{0, 0, 0}
Boundary condition	Wall functions
Use weak constraints	Off
Apply wall roughness	Off

1.4.3 Initial Values 1



Initial Values 1

Selection

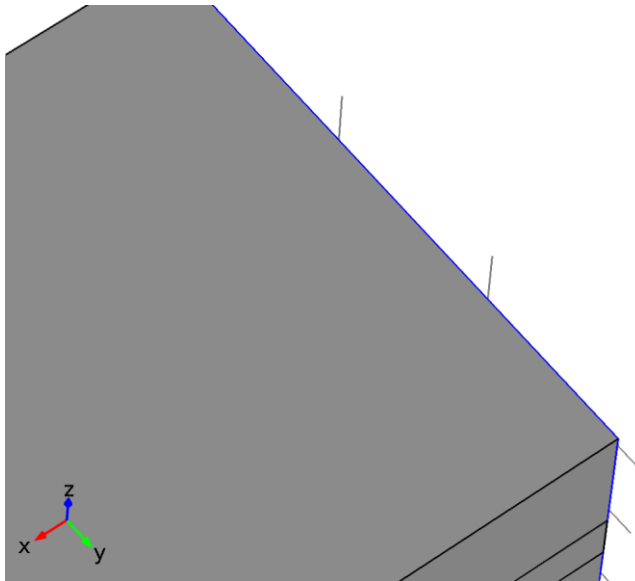
Geometric entity level	Domain
Selection	Domains 1–2

Settings

Settings

Description	Value
Velocity field	{0, 0, 0}
Pressure	0
Turbulent kinetic energy	spf.kinit
Turbulent dissipation rate	spf.epinit

1.4.4 Inlet 1



Inlet 1

Selection

Geometric entity level	Boundary
Selection	Boundaries 1, 7

Equations

$$\mathbf{u} = -U_0 \mathbf{n}$$

$$k = \frac{3}{2}(U_0 / L_T)^2, \quad \epsilon = C_\mu \frac{k^{3/2}}{L_T}$$

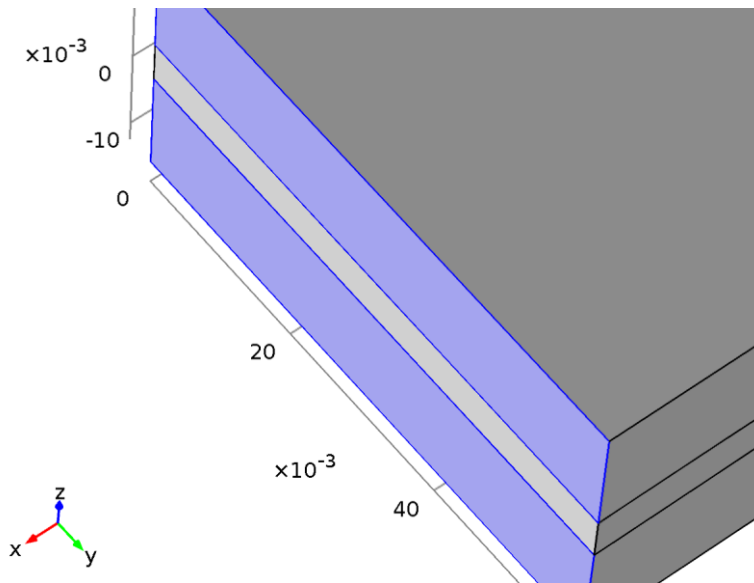
Settings

Settings

Description	Value
Apply reaction terms on	All physics (symmetric)
Use weak constraints	Off
Boundary condition	Velocity
Velocity field componentwise	Normal inflow velocity
Normal inflow velocity	0.5
Standard pressure	1[atm]
Standard molar volume	0.0224136[m ³ /mol]
Normal mass flow rate	1e-5[kg/s]
Mass flow type	Mass flow rate
Standard flow rate defined by	Standard density

Description	Value
	Specify turbulent length scale and intensity
Turbulent intensity	0.05
Turbulence length scale	0.01[m]

1.4.5 Outlet 1



Outlet 1

Selection

Geometric entity level	Boundary
Selection	Boundaries 230, 232

Equations

$$\underline{\mathbf{u}} = U_0 \mathbf{n}$$

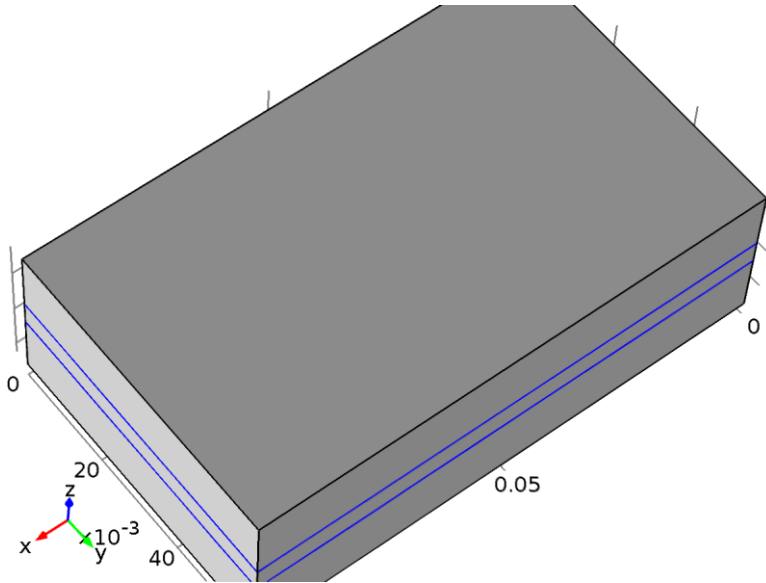
$$\nabla k \cdot \mathbf{n} = 0, \quad \nabla \epsilon \cdot \mathbf{n} = 0$$

Settings

Settings

Description	Value
Boundary condition	Velocity
Velocity field componentwise	Normal outflow velocity
Normal outflow velocity	0.5
Apply reaction terms on	All physics (symmetric)
Use weak constraints	Off

1.4.6 Interior Wall 1



Interior Wall 1

Selection

Geometric entity level	Boundary
Selection	Boundaries 6, 9, 14–229

Equations

$$\underline{\mathbf{u}}_u \cdot \mathbf{n} = 0$$

$$\left[(\mu_u + \mu_{T,u}) (\nabla \underline{\mathbf{u}}_u + (\nabla \underline{\mathbf{u}}_u)^T) - \frac{2}{3} (\mu_u + \mu_{T,u}) (\nabla \cdot \underline{\mathbf{u}}_u) \mathbf{I} - \frac{2}{3} \rho_u k_u \mathbf{I} \right] \cdot (-\mathbf{n}) = -\rho_u \frac{u_{\tau u}}{\delta_{w,u}^+} \underline{\mathbf{u}}_{\text{tang},u}$$

$$\underline{\mathbf{u}}_{\text{tang},u} = \underline{\mathbf{u}}_u - (\underline{\mathbf{u}}_u \cdot \mathbf{n}) \mathbf{n}$$

$$\nabla k_u \cdot \mathbf{n} = 0, \quad \epsilon_u = -\rho_u \frac{C_\mu k_u^2}{K_\nu \delta_{w,u}^+ \mu_u}$$

$$\underline{\mathbf{u}}_d \cdot \mathbf{n} = 0$$

$$\left[(\mu_d + \mu_{T,d}) (\nabla \underline{\mathbf{u}}_d + (\nabla \underline{\mathbf{u}}_d)^T) - \frac{2}{3} (\mu_d + \mu_{T,d}) (\nabla \cdot \underline{\mathbf{u}}_d) \mathbf{I} - \frac{2}{3} \rho_d k_d \mathbf{I} \right] \cdot \mathbf{n} = -\rho_d \frac{u_{\tau d}}{\delta_{w,d}^+} \underline{\mathbf{u}}_{\text{tang},d}$$

$$\underline{\mathbf{u}}_{\text{tang},d} = \underline{\mathbf{u}}_d - (\underline{\mathbf{u}}_d \cdot \mathbf{n}) \mathbf{n}$$

$$\nabla k_d \cdot \mathbf{n} = 0, \quad \epsilon_d = -\rho_d \frac{C_\mu k_d^2}{K_\nu \delta_{w,d}^+ \mu_d}$$

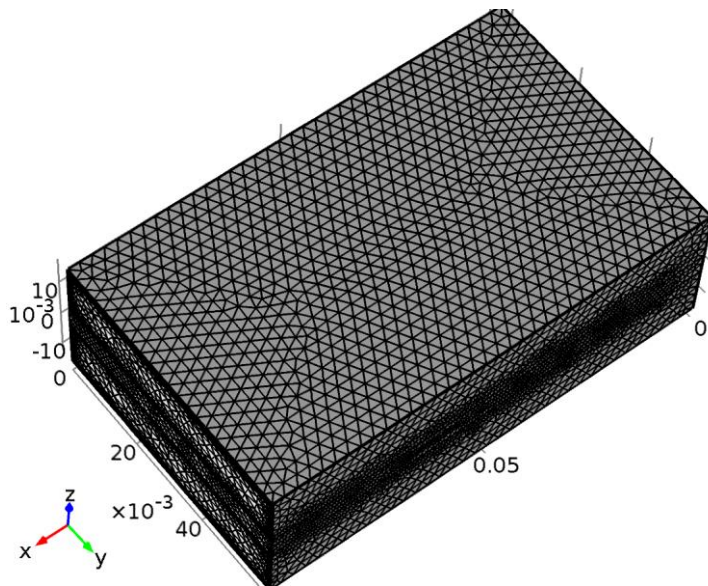
Settings

Settings

Description	Value
Temperature	User defined
Temperature	293.15[K]
Electric field	User defined

Description	Value
Electric field	{0, 0, 0}
Boundary condition	Wall functions
Apply wall roughness	On
Roughness model	Sand roughness
Equivalent sand roughness height	3.2[um]
Apply reaction terms on	All physics (symmetric)

1.5 Mesh 1



Mesh 1

1.5.1 Size (size)

Settings

Name	Value
Calibrate for	Fluid dynamics
Maximum element size	0.00552
Minimum element size	0.0017
Curvature factor	0.8
Resolution of narrow regions	0.5
Maximum element growth rate	1.25
Predefined size	Coarser

2 Study 1

2.1 Stationary

Study settings

Property	Value
Include geometric nonlinearity	Off

Mesh selection

Geometry	Mesh
Geometry 1 (geom1)	mesh1

Physics selection

Physics	Discretization
Turbulent Flow, k-ε (spf)	physics

2.2 Solver Configurations

2.2.1 Solver 1

Compile Equations: Stationary (st1)

Study and step

Name	Value
Use study	Study 1
Use study step	Stationary

Dependent Variables 1 (v1)

General

Name	Value
Defined by study step	Stationary

Initial values of variables solved for

Name	Value
Solution	Zero

Values of variables not solved for

Name	Value
Solution	Zero

Pressure (comp1.p) (comp1_p)

General

Name	Value
Field components	comp1.p

Turbulent dissipation rate (comp1.ep) (comp1_ep)

General

Name	Value
Field components	comp1.ep

Turbulent kinetic energy (comp1.k) (comp1_k)

General

Name	Value
Field components	comp1.k

Velocity field (comp1.u) (comp1_u)

General

Name	Value
Field components	{comp1.u, comp1.v, comp1.w}

Stationary Solver 1 (s1)

General

Name	Value
Defined by study step	Stationary

Segregated 1 (se1)

General

Name	Value
Pseudo time-stepping	On
Initial CFL number	3

Segregated Step 1 (ss1)

General

Name	Value
Variables	{Velocity field (comp1.u), Pressure (comp1.p)}
Linear solver	Iterative 1

Segregated Step 2 (ss2)

General

Name	Value
Variables	{Turbulent kinetic energy (comp1.k), Turbulent dissipation rate (comp1.ep)}
Linear solver	Iterative 2

Lower Limit 1 (ll1)

Lower limit

Name	Value
Lower limits (field variables)	comp1.k 0 comp1.ep 0

Iterative 1 (i1)

Error

Name	Value
Factor in error estimate	20
Maximum number of iterations	200
Nonlinear based error norm	On

Multigrid 1 (mg1)

Coarse Solver (cs)

Direct 1 (d1)

General

Name	Value
Solver	PARDISO

Iterative 2 (i2)

Error

Name	Value
Maximum number of iterations	200
Nonlinear based error norm	On

Multigrid 1 (mg1)

Presmoothing (pr)

SOR Line 1 (sl1)

Main

Name	Value
Number of iterations	1
Relaxation factor	0.2

Secondary

Name	Value
Number of secondary iterations	2
Relaxation factor	0.5

Postsmoother (po)

SOR Line 1 (sl1)

Main

Name	Value
Relaxation factor	0.2

Secondary

Name	Value
Number of secondary iterations	2
Relaxation factor	0.5

Coarse Solver (cs)

Direct 1 (d1)

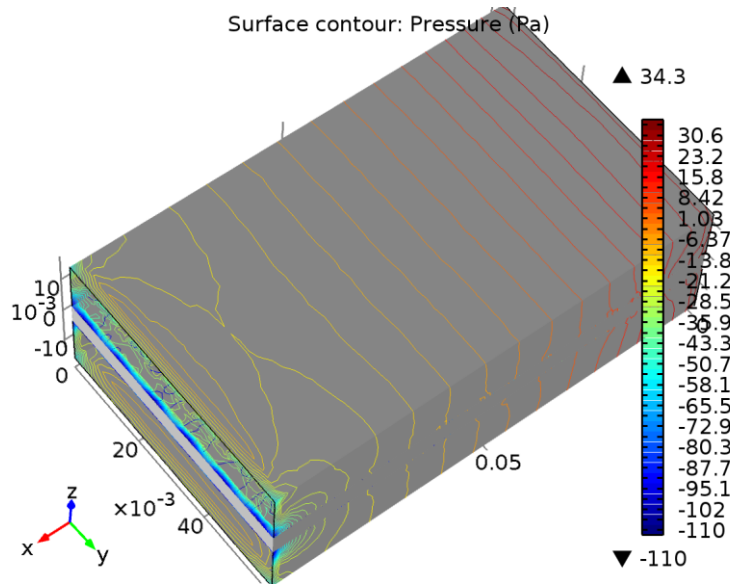
General

Name	Value
Solver	PARDISO

3 Results

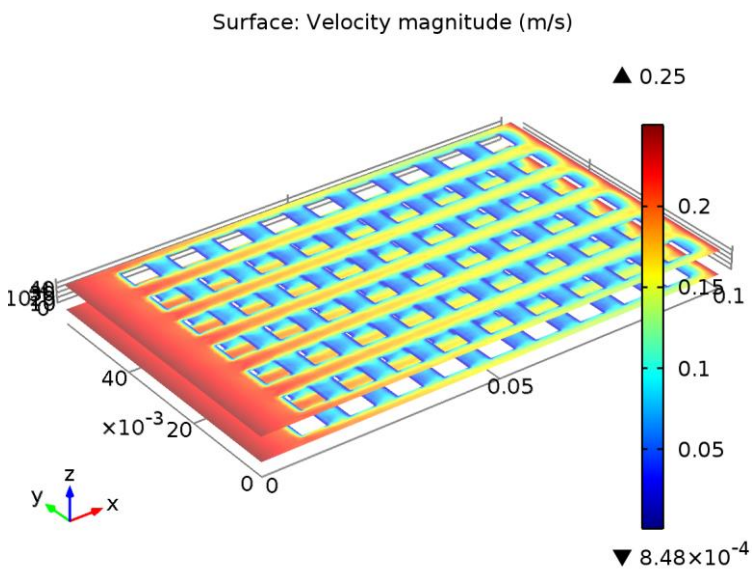
3.1 Plot Groups

3.1.1 Pressure (spf)



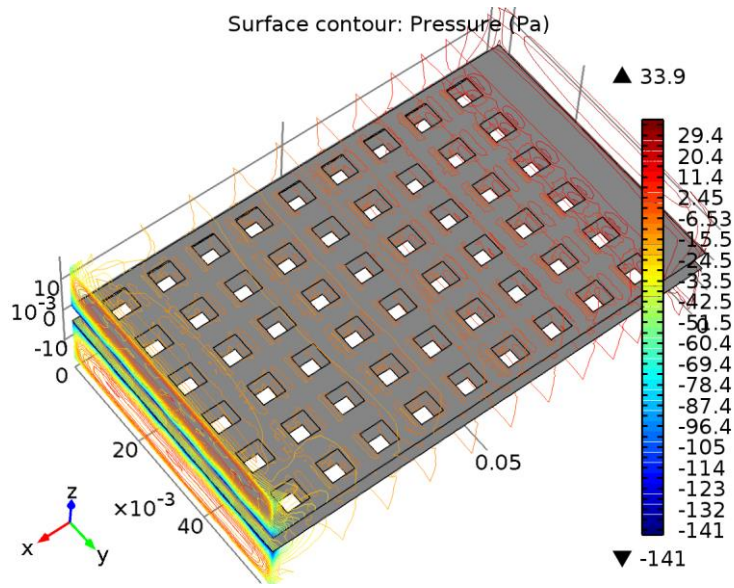
Surface contour: Pressure (Pa)

3.1.2 Velocity (spf) 1



Streamline: Velocity field Surface: Velocity magnitude (m/s)

3.1.3 Pressure (spf) 1



Surface contour: Pressure (Pa)

B- COMSOL, spraying phase

1. Component 1 (comp1)	37
1.1. Definitions	37
1.2. Geometry 1	37
1.3. Materials	38
1.4. Turbulent Flow, k- ϵ (spf)	39
1.5. Mesh 1	46
2. Study 1	47
2.1. Stationary	47
2.2. Solver Configurations	47
3. Results	51
3.1. Plot Groups	51

1 Component 1 (comp1)

1.1 Definitions

1.1.1 Coordinate Systems

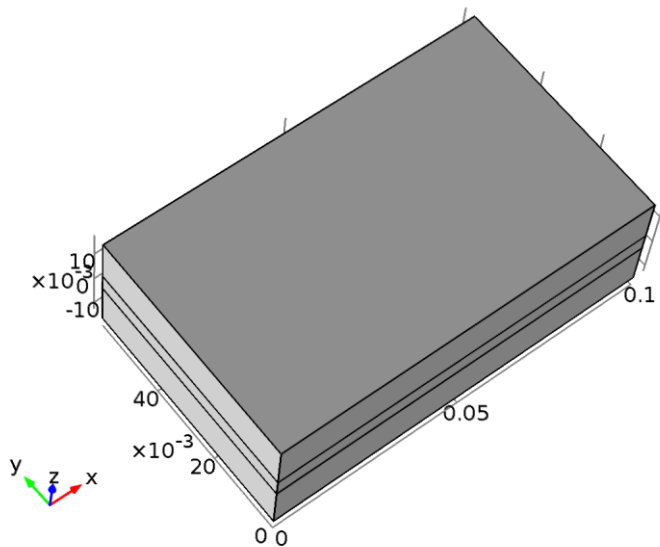
Boundary System 1

Coordinate system type	Boundary system
Identifier	sys1

Settings

Name	Value
Coordinate names	{t1, t2, n}
Create first tangent direction from	Global Cartesian

1.2 Geometry 1



Geometry 1

Units

Length unit	m
Angular unit	deg

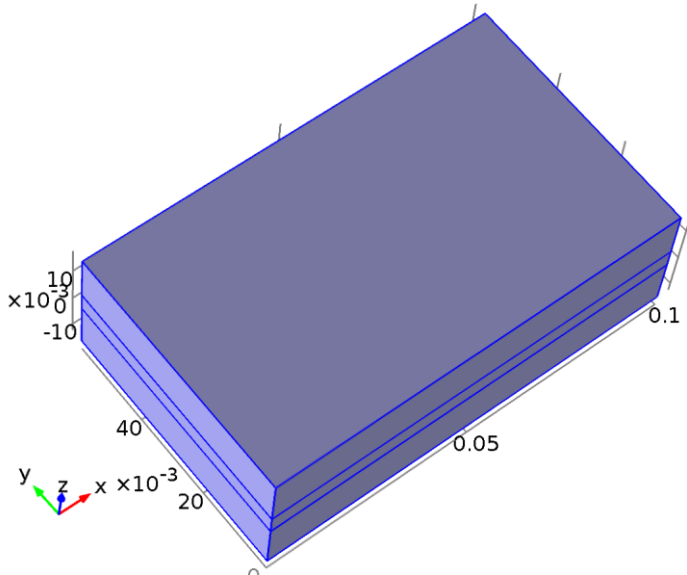
Geometry statistics

Property	Value
Space dimension	3
Number of domains	2
Number of boundaries	232

Property	Value
Number of edges	676
Number of vertices	448

1.3 Materials

1.3.1 Water



Water

Selection

Geometric entity level	Domain
Selection	Domains 1–2

Material parameters

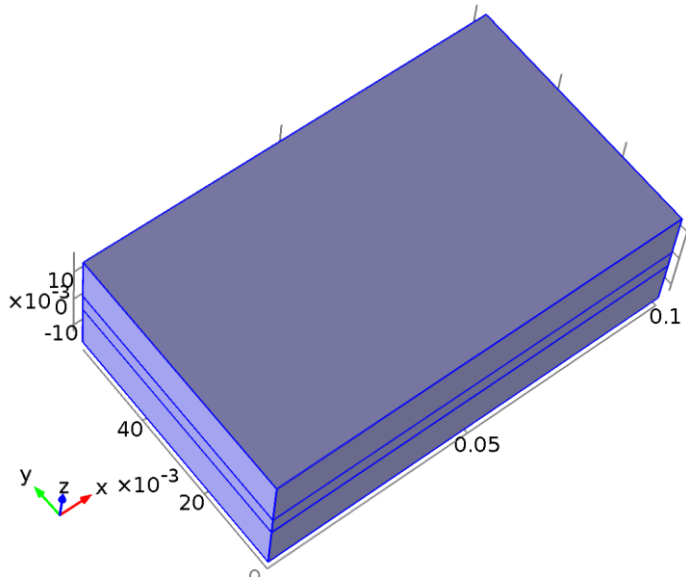
Name	Value	Unit
Dynamic viscosity	$\eta(T[1/K])[\text{Pa}\cdot\text{s}]$	$\text{Pa}\cdot\text{s}$
Density	$\rho(T[1/K])[\text{kg}/\text{m}^3]$	kg/m^3

Basic Settings

Description	Value
Dynamic viscosity	$\eta(T[1/K])[\text{Pa}\cdot\text{s}]$
Ratio of specific heats	1.0
Electrical conductivity	$\{\{5.5\text{e-}6[\text{S}/\text{m}], 0, 0\}, \{0, 5.5\text{e-}6[\text{S}/\text{m}], 0\}, \{0, 0, 5.5\text{e-}6[\text{S}/\text{m}]\}\}$
Heat capacity at constant pressure	$C_p(T[1/K])[\text{J}/(\text{kg}\cdot\text{K})]$
Density	$\rho(T[1/K])[\text{kg}/\text{m}^3]$

Description	Value
Thermal conductivity	{{k(T[1/K])[W/(m*K)], 0, 0}, {0, k(T[1/K])[W/(m*K)], 0}, {0, 0, k(T[1/K])[W/(m*K)]}}
Speed of sound	cs(T[1/K])[m/s]

1.4 Turbulent Flow, k-ε (spf)



Turbulent Flow, k-ε

Selection

Geometric entity level	Domain
Selection	Domains 1–2

Equations

$$\rho(\mathbf{u} \cdot \nabla)\mathbf{u} = \nabla \cdot \left[-p\mathbf{I} + \left(\mu + \mu_T \right) (\nabla\mathbf{u} + (\nabla\mathbf{u})^T) - \frac{2}{3}(\mu + \mu_T)(\nabla \cdot \mathbf{u})\mathbf{I} - \frac{2}{3}\rho k\mathbf{I} \right] + \mathbf{F}$$

$$\nabla \cdot (\rho\mathbf{u}) = 0$$

$$\rho(\mathbf{u} \cdot \nabla)k = \nabla \cdot \left[\left(\mu + \frac{\mu_T}{\sigma_k} \right) \nabla k \right] + P_k - \rho\varepsilon$$

$$\rho(\mathbf{u} \cdot \nabla)\varepsilon = \nabla \cdot \left[\left(\mu + \frac{\mu_T}{\sigma_\varepsilon} \right) \nabla \varepsilon \right] + C_{d1} \frac{\varepsilon}{k} P_k - C_{d2} \rho \frac{\varepsilon^2}{k}, \quad \varepsilon = \varepsilon_p$$

$$\mu_T = \rho C_\mu \frac{k^2}{\varepsilon}$$

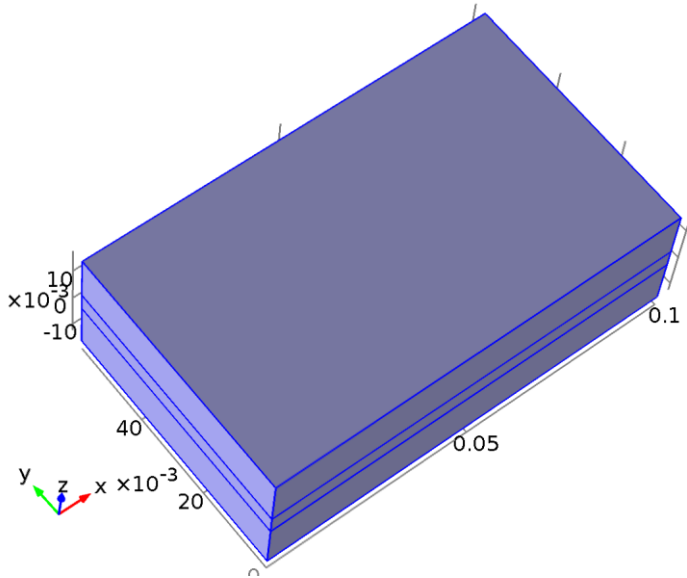
$$P_k = \mu_T \left[\nabla\mathbf{u} : (\nabla\mathbf{u} + (\nabla\mathbf{u})^T) - \frac{2}{3}(\nabla \cdot \mathbf{u})^2 \right] - \frac{2}{3}\rho k \nabla \cdot \mathbf{u}$$

Settings

Description	Value
Discretization of fluids	P1 + P1

Description	Value
Value type when using splitting of complex variables	{Real, Real, Real, Real, Real, Real, Real, Real, Real}

1.4.1 Fluid Properties 1



Fluid Properties 1

Selection

Geometric entity level	Domain
Selection	Domains 1–2

Equations

$$\rho(\mathbf{u} \cdot \nabla)\mathbf{u} = \nabla \cdot \left[-p\mathbf{I} + (\mu + \mu_T)(\nabla\mathbf{u} + (\nabla\mathbf{u})^T) - \frac{2}{3}(\mu + \mu_T)(\nabla \cdot \mathbf{u})\mathbf{I} - \frac{2}{3}\rho k\mathbf{I} \right] + \mathbf{F}$$

$$\nabla \cdot (\rho\mathbf{u}) = 0$$

$$\rho(\mathbf{u} \cdot \nabla)k = \nabla \cdot \left[\left(\mu + \frac{\mu_T}{\sigma_k} \right) \nabla k \right] + P_k - \rho\epsilon$$

$$\rho(\mathbf{u} \cdot \nabla)\epsilon = \nabla \cdot \left[\left(\mu + \frac{\mu_T}{\sigma_\epsilon} \right) \nabla \epsilon \right] + C_{\epsilon 1} \frac{\epsilon}{k} P_k - C_{\epsilon 2} \rho \frac{\epsilon^2}{k}, \quad \epsilon = \text{ep}$$

Settings

Settings

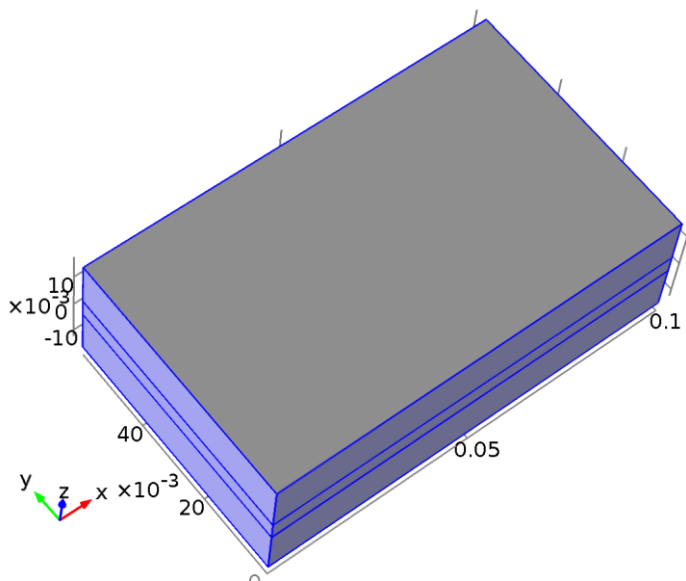
Description	Value
Density	From material
Dynamic viscosity	From material
Reference length	1

Description	Value
Reference length scale	Automatic
Mixing length limit	Automatic

Properties from material

Property	Material	Property group
Density	Water	Basic
Dynamic viscosity	Water	Basic

1.4.2 Wall 1



Wall 1

Selection

Geometric entity level	Boundary
Selection	Boundaries 1–2, 4–5, 7–8, 11–13, 230–232

Equations

$$\underline{\mathbf{u}} \cdot \mathbf{n} = 0$$

$$\left[(\mu + \mu_T)(\nabla \mathbf{u} + (\nabla \mathbf{u})^T) - \frac{2}{3}(\mu + \mu_T)(\nabla \cdot \mathbf{u})\mathbf{I} - \frac{2}{3}\rho k\mathbf{I} \right] \mathbf{n} = -\rho \frac{u_\tau}{\delta_w^+} \mathbf{u}_{\text{tang}}$$

$$\mathbf{u}_{\text{tang}} = \mathbf{u} - (\mathbf{u} \cdot \mathbf{n})\mathbf{n}$$

$$\nabla k \cdot \mathbf{n} = 0, \quad \epsilon = \rho \frac{C_\mu k^2}{K_\nu \delta_w^+ \mu}$$

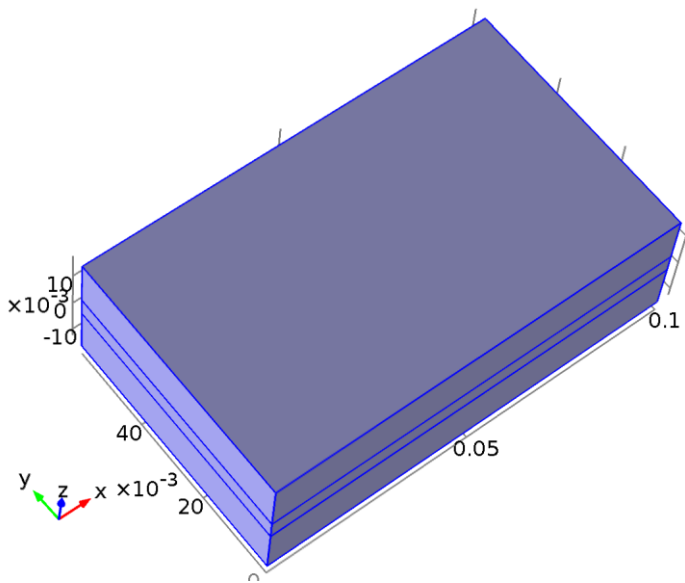
Settings

Settings

Description	Value
-------------	-------

Description	Value
Temperature	User defined
Temperature	293.15[K]
Electric field	User defined
Electric field	{0, 0, 0}
Boundary condition	Wall functions
Use weak constraints	Off
Apply wall roughness	Off

1.4.3 Initial Values 1



Initial Values 1

Selection

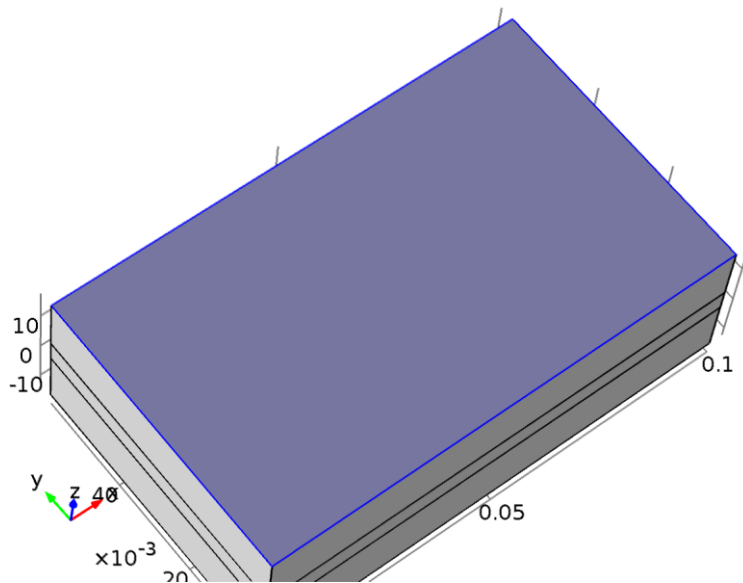
Geometric entity level	Domain
Selection	Domains 1–2

Settings

Settings

Description	Value
Velocity field	{0, 0, 0}
Pressure	0
Turbulent kinetic energy	spf.kinit
Turbulent dissipation rate	spf.epinit

1.4.4 Inlet 1



Inlet 1

Selection

Geometric entity level	Boundary
Selection	Boundary 10

Equations

$$\mathbf{u} = -U_0 \mathbf{n}$$

$$k = \frac{3}{2}(U_0/L_T)^2, \quad \epsilon = C_\mu \frac{3/4 k^{3/2}}{L_T}$$

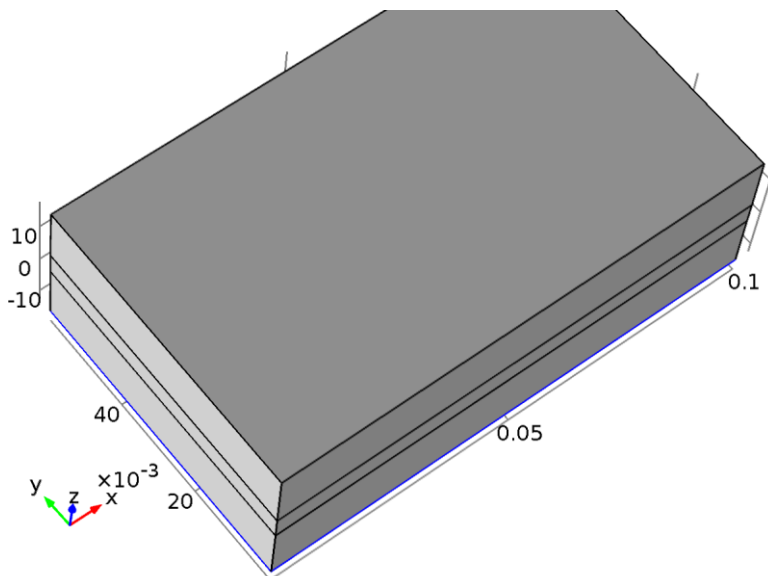
Settings

Settings

Description	Value
Apply reaction terms on	All physics (symmetric)
Use weak constraints	Off
Boundary condition	Velocity
Velocity field componentwise	Normal inflow velocity
Normal inflow velocity	0.5
Standard pressure	1[atm]
Standard molar volume	0.0224136[m ³ /mol]
Normal mass flow rate	1e-5[kg/s]
Mass flow type	Mass flow rate
Standard flow rate defined by	Standard density

Description	Value
	Specify turbulent length scale and intensity
Turbulent intensity	0.05
Turbulence length scale	0.01[m]

1.4.5 Outlet 1



Outlet 1

Selection

Geometric entity level	Boundary
Selection	Boundary 3

Equations

$$\mathbf{u} = U_0 \mathbf{n}$$

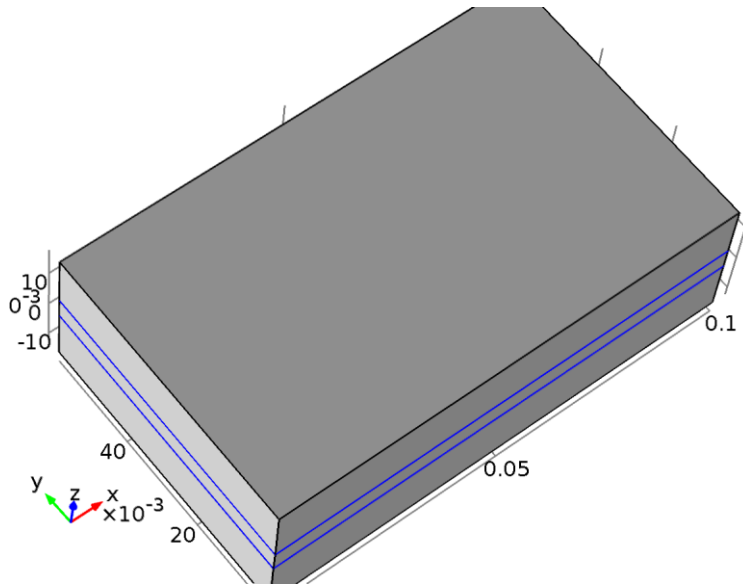
$$\nabla k \cdot \mathbf{n} = 0, \quad \nabla \epsilon \cdot \mathbf{n} = 0$$

Settings

Settings

Description	Value
Boundary condition	Velocity
Velocity field componentwise	Normal outflow velocity
Normal outflow velocity	0.5
Apply reaction terms on	All physics (symmetric)
Use weak constraints	Off

1.4.6 Interior Wall 1



Interior Wall 1

Selection

Geometric entity level	Boundary
Selection	Boundaries 6, 9, 14–229

Equations

$$\begin{aligned} & \underline{\mathbf{u}}_u \cdot \mathbf{n} = 0 \\ & \left[(\mu_u + \mu_{T,u}) (\nabla \mathbf{u}_u + (\nabla \mathbf{u}_u)^T) - \frac{2}{3} (\mu_u + \mu_{T,u}) (\nabla \cdot \mathbf{u}_u) \mathbf{I} - \frac{2}{3} \rho_u k_u \mathbf{I} \right] \cdot \mathbf{n} = -\rho_u \frac{u_{\tau u}}{\delta_{w,u}^+} \mathbf{u}_{\text{tang},u} \\ & \mathbf{u}_{\text{tang},u} = \mathbf{u}_u - (\mathbf{u}_u \cdot \mathbf{n}) \mathbf{n} \\ & \nabla k_u \cdot \mathbf{n} = 0, \quad \epsilon_u = -\rho_u \frac{C_\mu k_u^2}{k_v \delta_{w,u}^+ \mu_u} \\ & \underline{\mathbf{u}}_d \cdot \mathbf{n} = 0 \\ & \left[(\mu_d + \mu_{T,d}) (\nabla \mathbf{u}_d + (\nabla \mathbf{u}_d)^T) - \frac{2}{3} (\mu_d + \mu_{T,d}) (\nabla \cdot \mathbf{u}_d) \mathbf{I} - \frac{2}{3} \rho_d k_d \mathbf{I} \right] \cdot \mathbf{n} = -\rho_d \frac{u_{\tau d}}{\delta_{w,d}^+} \mathbf{u}_{\text{tang},d} \\ & \mathbf{u}_{\text{tang},d} = \mathbf{u}_d - (\mathbf{u}_d \cdot \mathbf{n}) \mathbf{n} \\ & \nabla k_d \cdot \mathbf{n} = 0, \quad \epsilon_d = -\rho_d \frac{C_\mu k_d^2}{k_v \delta_{w,d}^+ \mu_d} \end{aligned}$$

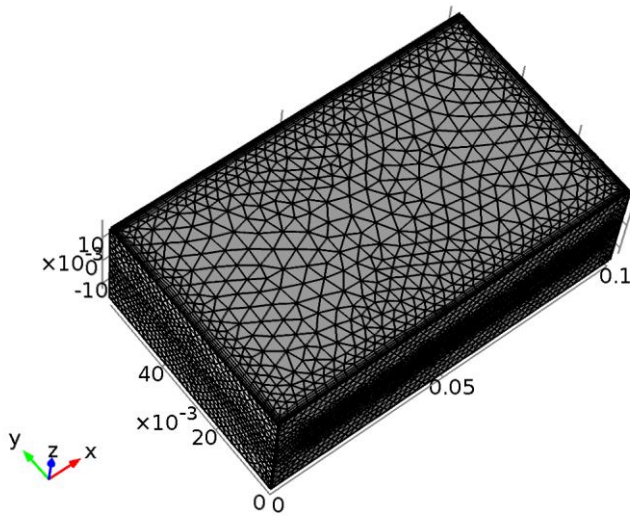
Settings

Settings

Description	Value
Temperature	User defined
Temperature	293.15[K]
Electric field	User defined

Description	Value
Electric field	{0, 0, 0}
Boundary condition	Wall functions
Apply wall roughness	On
Roughness model	Sand roughness
Equivalent sand roughness height	3.2[um]
Apply reaction terms on	All physics (symmetric)

1.5 Mesh 1



Mesh 1

1.5.1 Size (size)

Settings

Name	Value
Calibrate for	Fluid dynamics
Maximum element size	0.00552
Minimum element size	0.0017
Curvature factor	0.8
Resolution of narrow regions	0.5
Maximum element growth rate	1.25
Predefined size	Coarser

2 Study 1

2.1 Stationary

Study settings

Property	Value
Include geometric nonlinearity	Off

Mesh selection

Geometry	Mesh
Geometry 1 (geom1)	mesh1

Physics selection

Physics	Discretization
Turbulent Flow, k- ϵ (spf)	physics

2.2 Solver Configurations

2.2.1 Solver 1

Compile Equations: Stationary (st1)

Study and step

Name	Value
Use study	Study 1
Use study step	Stationary

Dependent Variables 1 (v1)

General

Name	Value
Defined by study step	Stationary

Initial values of variables solved for

Name	Value
Solution	Zero

Values of variables not solved for

Name	Value
Solution	Zero

Pressure (comp1.p) (comp1_p)

General

Name	Value
Field components	comp1.p

Turbulent dissipation rate (comp1.ep) (comp1_ep)

General

Name	Value
Field components	comp1.ep

Turbulent kinetic energy (comp1.k) (comp1_k)

General

Name	Value
Field components	comp1.k

Velocity field (comp1.u) (comp1_u)

General

Name	Value
Field components	{comp1.u, comp1.v, comp1.w}

Stationary Solver 1 (s1)

General

Name	Value
Defined by study step	Stationary

Segregated 1 (se1)

General

Name	Value
Pseudo time-stepping	On
Initial CFL number	3

Segregated Step 1 (ss1)

General

Name	Value
Variables	{Velocity field (comp1.u), Pressure (comp1.p)}
Linear solver	Iterative 1

Segregated Step 2 (ss2)

General

Name	Value

Name	Value
Variables	{Turbulent kinetic energy (comp1.k), Turbulent dissipation rate (comp1.ep)}
Linear solver	Iterative 2

Lower Limit 1 (ll1)

Lower limit

Name	Value
Lower limits (field variables)	comp1.k 0 comp1.ep 0

Iterative 1 (i1)

Error

Name	Value
Factor in error estimate	20
Maximum number of iterations	200
Nonlinear based error norm	On

Multigrid 1 (mg1)

Coarse Solver (cs)

Direct 1 (d1)

General

Name	Value
Solver	PARDISO

Iterative 2 (i2)

Error

Name	Value
Maximum number of iterations	200
Nonlinear based error norm	On

Multigrid 1 (mg1)

Presmoothing (pr)

SOR Line 1 (sl1)

Main

Name	Value
Number of iterations	1
Relaxation factor	0.2

Secondary

Name	Value
Number of secondary iterations	2
Relaxation factor	0.5

Postsmoother (po)

SOR Line 1 (sl1)

Main

Name	Value
Relaxation factor	0.2

Secondary

Name	Value
Number of secondary iterations	2
Relaxation factor	0.5

Coarse Solver (cs)

Direct 1 (d1)

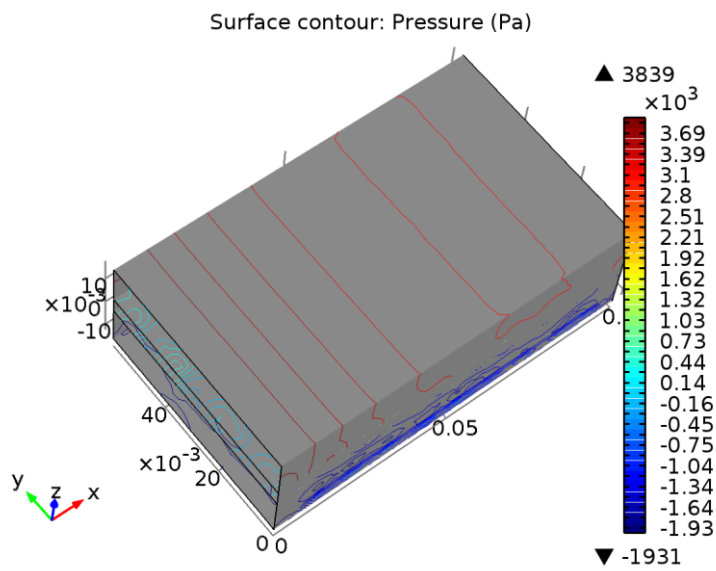
General

Name	Value
Solver	PARDISO

3 Results

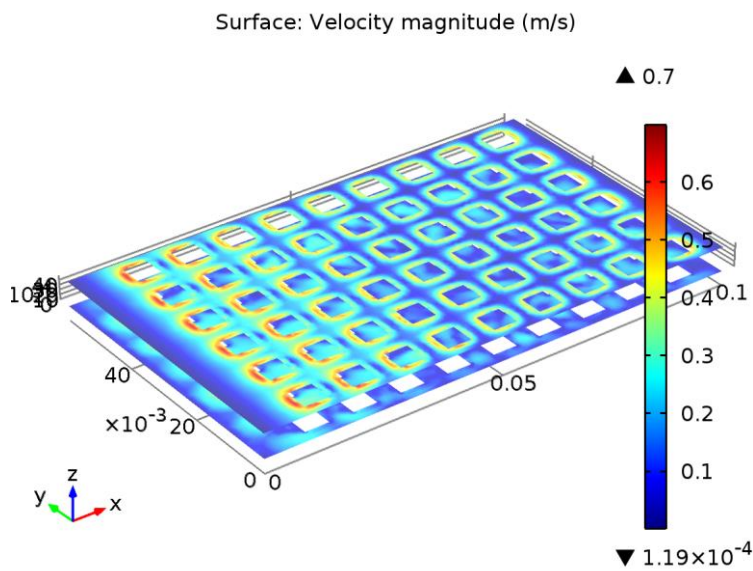
3.1 Plot Groups

3.1.1 Pressure (spf)



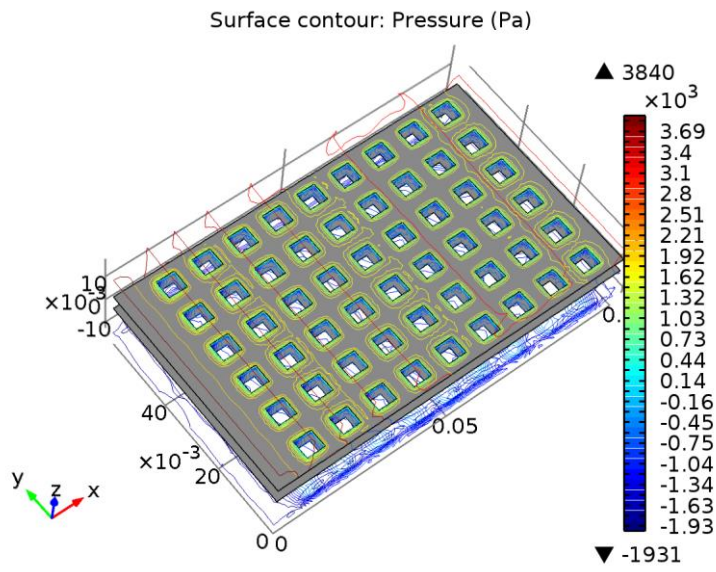
Surface contour: Pressure (Pa)

3.1.2 Velocity (spf) 1



Streamline: Velocity field Surface: Velocity magnitude (m/s)

3.1.3 Pressure (spf) 1



Surface contour: Pressure (Pa)